RSC Advances

ROYAL SOCIETY OF CHEMISTRY

www.rsc.org/advances

RSC Advances

RSCPublishing

Paper

Limitation factors for the performance of kesterite Cu_2ZnSnS_4 thin film solar cells studied by defects characterization

Cite this: DOI: 10.1039/xoxxoooooox

Received ooth XX 2015,
Accepted ooth XX 2015

DOI: 10.1039/xoxxoooooox

www.rsc.org/

Ling Yin,[ab] Guanming Cheng,[b] Ye Feng,[b] Zhaohui Li,[b] Chunlei Yang,*[b] Xudong Xiao*[ab]

In this work, photoluminescence (PL), admittance spectroscopy (AS) and drive-level capacitance profiling (DLCP) were performed to analyze the defect properties of a Cu_2ZnSnS_4 (CZTS) solar cell. Comparing to a high efficiency $CuInGaSe_2$ (CIGS) solar cell, the absorber of the CTZS device has larger potential fluctuation which can be attributed to the co-existence of high concentration deep acceptor (Cu_{Zn}) and deep donor (Zn_{Cu}) defects. The density of the interface states in the CZTS device is also orders higher than that in the CIGS device. These high density defects (both in the bulk and at the CZTS/CdS interface) will induce a large loss in the open-circuit voltage (V_{oc}), resulting in a lower performance of the CZTS device. We suggest that defect control can be a possible solution to reduce the potential fluctuation induced by acceptors. To overcome the potential fluctuation induced trapping effect for electrons by the Zn_{Cu} donors, a graded conduction band similar to CIGS will be good to eliminate electron localization.

1. Introduction

Kesterite Cu_2ZnSnS_4 has drawn a lot of attention due to its ideal wide band gap, high absorption and the abundance of raw material.[1-3] In the past few years, various methods including sputtering, evaporation, spray pyrolysis, ink-based approaches and solution-based hydrazine process have been developed to fabricate CZTS devices.[3-9] The current record of the solar energy conversion efficiency of CZTSSe and pure CZTS solar cells are 12.6% (by IBM group) and 9.2% (by Solar Frontier K. K.), respectively.[10,11] However they are still much lower than the CIGS record 21.7% (by ZSW).[12] To further improve the conversion efficiency of CZTS-based solar cells, it is important to get more detailed information about the optoelectronic properties of CZTS-based materials and understand the key factors which limit the CZTS-based solar cell performance. Recently, Tayfun Gokmen et al. demonstrated that the formation of band-edge tail states is a fundamental performance bottleneck for hydrazine processed CZTSSe solar cells.[13] However, the limitation factor for the performance of CZTS solar cells is still an open question.

Photoluminescence (PL) spectrum is a powerful optical method for the characterization of solar cells. From the PL spectrum, important information about the radiative and nonradiative recombination can be obtained.[14] The PL emissions in CZTS and CIGS involving tail states transitions usually show asymmetrical PL bands. By fitting these asymmetrical PL spectrum, either using the Gaussian-like defect model or the exponential-like tail model, average energy depth of the potential fluctuations can be extracted.[15-16] Since the potential fluctuations usually act as potential traps for carriers, the energy depth of the potential fluctuations will be a critical factor in limiting the transport/diffusion of photo-induced carriers in a semiconductor thin film. J. H. Werner et al. reported that the potential fluctuations reduce the efficiency of CIGS solar cells,[17] and S. Siebentritt et al. also found that the potential fluctuations become deeper with increasing stoichiometric deviation in CIGS solar cells.[16] Intensity-dependent PL measurement at low temperature can be used to estimate the quasi donor-acceptor pair defect density. By this method, Talia Gershon et al. concluded that the total defect density is a better indicator of CZTS device efficiency than the starting metal ratios alone.[18]

Admittance spectroscopy (AS) is another important solar cell characterization technique which allows insight into the energetic position and the density of states of the defects. The technique is based on the analysis of capacitance measured as a function of frequency and temperature. On the other hand, as reported by Heath et al, the drive level capacitance profiling (DLCP) measurement is a useful technique enabling the

[a] *Department of Physics, The Chinese University of Hong Kong, Shatin, Hong Kong, China. Email: xdxiao@phy.cuhk.edu.hk*

[b] *Center for Photovoltaics and Solar Energy, Shenzhen Institutes of Advanced Technology, Chinese Academy of Sciences, Shenzhen, 518055, P. R. China. Email: cl.yang@siat.ac.cn*

identification of net carrier and different type of defects, including bulk defect and interface defect in thin films.[19] As for the record CZTS-based solar cell, the drive level density measured by DLCP is less than 7×10^{15} cm^{-3}, similar with the value of a higher efficiency CIGS solar cell.[10]

In previous work, the potential fluctuation or tail states were demonstrated mainly by studying the optical properties such as absorption and photoluminescence spectra. In this work, in addition to the optical techniques, we have also used admittance spectra to show the effect of potential fluctuation by revealing its trapping process on the carrier transport in CZTS and CIGS devices. We believe the trapping potential measured by the admittance measurement will be more directly related to the device performance. The trapping energy will also be very helpful in identifying the possible origin of the defects contributing to the potential fluctuation. By using DLCP, we further show that the much higher density of interface stages is another origin for the voltage loss in CZTS by comparing with CIGS.

2. Experimental

The solar cells investigated in this paper consist of Ni-Al-Ni/AZO/ZnO/CdS /(CZTS or CIGS)/Mo layers deposited on soda-lime glass (SLG). The absorber of the CZTS cell (with efficiency 6.25%) was fabricated by sulfurization of co-sputtered SnS_2-ZnS-Cu precursor and the composition (Cu/Zn=1.15, Zn/Sn=1.35) is determined by Energy Dispersive X-Ray Spectroscopy (EDX). The reference CIGS sample (with efficiency 19.4%) was deposited by three-stage evaporation with a V-shape Ga/[In+Ga] profile across the absorber. The averaged Ga/[In+Ga] across the absorber is about 0.32, while the surface Ga/[In+Ga] ratio is about 0.36. The values of bandgap of both CIGS and CZTS absorber layers are estimated from the absorption edges using the inflection of the external quantum efficiency (EQE) curves near the band edges.[13]

The PL measurement was performed by mounting the devices in a close-cycled cryostat with which the temperature can be varied in the range of 10–400 K. The 633 nm Helium-neon gas laser was used as the excitation source and the emission signals were detected by a HORIBA iHR550 spectrometer equipped with a CCD detector cooled at -80 °C. The AS measurement was conducted in the dark and the capacitance was measured in the frequency range from 100 Hz to 1MHz, with an oscillating voltage of 30 mV. The DLCP was measured at different frequency with ac excitations of amplitude varied from 20 to 200 mV. Finally, the current-voltage (IV) characteristics of the devices were measured using an solar simulator with an Keithley 2400 source meter under illumination intensity of 100 mW/cm^2.

3. Results and discussion

The performances of the CZTS and CIGS solar cells are listed in Table 1. The bandgap of the CZTS absorber is about 0.3 eV larger than the surface bandgap of the CIGS absorber, while the

Table 1. IV performance of CZTS and CIGS solar cells

Sample	Bandgap (eV)	Voc (mV)	Jsc (mA/cm2)	FF %	η %
CZTS	1.510	623	15.7	63.9	6.25
CIGS	1.220	715	35.0	77.7	19.4

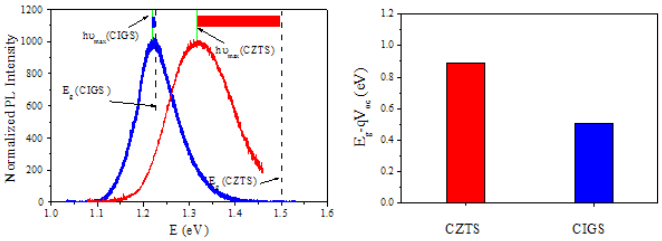

Fig. 1. (a) Room temperature PL spectroscopy of CZTS and CIGS. (b) Voc deficiency compared to bangdap in CZTS and CIGS.

V_{oc} of the CZTS solar cell is about 90mV lower than that of the CIGS solar cell. To study the V_{oc} deficiency problem in the CZTS solar cell, PL, AS and DLCP were employed to identify the different defect properties of the CZTS and CIGS solar cells. Fig. 1(a) shows the room temperature PL spectra of the CZTS and CIGS solar cells. The PL peaks of both solar cells are shifted to lower energies with respect to their bandgap energy Eg. However, the red shift of the PL peak relative to Eg for CIGS solar cell is relatively small (<5 meV) compared to that of the CZTS solar cell, which has a pronounced shift (~190 meV). In addition, the CZTS PL spectrum has a larger FWHM than that of the CIGS PL spectrum. E_g-qV_{oc}, the difference between the bandgap and qV_{oc} is plotted in Fig. 1(b). The CZTS solar cell has a larger V_{oc} deficit than that of the CIGS solar cell. This large V_{oc} deficiency in the CZTS in Fig. 1(b) is consistent with the pronounced red shift of the PL peak relative to Eg for CZTS device in Fig. 1(a). As indicated in the literature, a large red shift of the PL peak relative to Eg and the broadening of PL peaks can be often attributed to the potential fluctuations in CZTS absorber layers.[13,20,21] The tail states introduced by the potential fluctuation will reduce the effective bandgap of the absorber and thus decrease the V_{oc} of solar cells. To get more detailed information on the potential fluctuation, we have performed low temperature PL measurement since the carriers are intended to be trapped at those tail states when temperature is low. Fig. 2(a) shows the PL spectrum of the CZTS solar cell at 10 K. Compared to the PL spectrum measured at room temperature (Fig. 1(a)), the peak measured at 10 K shifts to lower energy. Two peaks located at 1.25 eV and 1.35 eV, respectively, are observed. Emission at lower energy can be attributed to carriers in localized states while the high energy emission involves states that are delocalized[18]. To estimate the potential fluctuation, we use the models developed by S. Siebentritt et. al,[16] in which the low-energy tail of the PL band due to fluctuations is treated either as defects (justified for deep enough fluctuations), and the density of states assumes a

Gaussian shape, or treated as Urbach tails, and the density of states shows an exponential decay.[15-16]

$$I(E)\sim\exp(-E/\gamma) \text{ or } I(E)\sim\exp(-(E-E_0)^2/2\gamma^2) \quad (1)$$

where E_0 is the average emission energy and γ is the fluctuating potentials. In Fig. 2(c), the low-energy tail of PL (red line) is fitted well with a Gaussian (blue dashed line), and the potential fluctuation γ for the CZTS solar cell in Eq. (1) is estimated to be 55.3 meV. We note that the potential fluctuations of the CZTS solar cells are almost three times larger than that of the CIGS solar cell listed in Table 2 (γ=16.7 meV), where the potential fluctuations of several chalcopyrite materials ($CuGaSe_2$ and $CuInSe_2$) are compared. The coincidence of the large potential fluctuation with large V_{oc} deficit is not only observed by comparing CZTS and CIGS device, but also observed by comparing various CZTS devices. We have used the same fitting method to deduce the potential fluctuation of a series of CZTS solar cells with efficiency ranging from 3.5% to 6.2%. Devices with smaller V_{oc} deficit are always found to be with smaller potential fluctuations. These results show that the value of potential fluctuation is one of the key factors limiting the performance of CZTS solar cells.

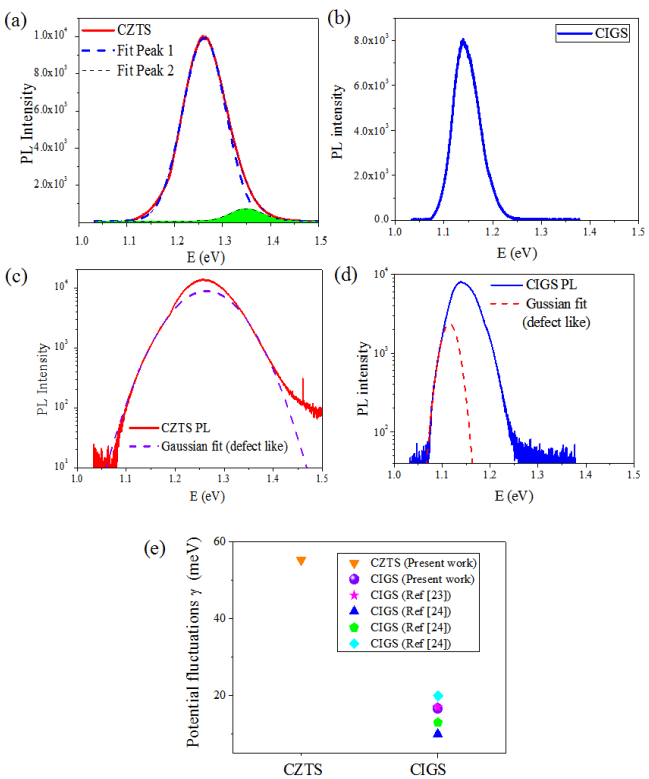

Fig. 2. (a) PL spectroscopy of CZTS at 10K. Two PL peaks are observed. (b) PL spectroscopy of CIGS at 10K. (c)-(d) CZTS and CIGS show Gaussian spectral dependence of the low-energy tail of emission. (e) Potential fluctuations values of CZTS and CIGS solar cells.

Table 2. Values of the potential fluctuations γ calculated from the low-energy tail of the PL band for CZTS and CIGS.

Compound	γ (meV)	FWHM (meV)	Reference
CZTS	55.3	105	Present work
CIGS	16.7	55	Present work
$CuGaSe_2$	17.6	50	[22]
$CuIn_{0.5}Ga_{0.5}Se_2$	17.0	49	[23]
$CuInGaSe_2$	10, 13, 20, 21	/	[24]
$CuInSe_2$	24.1	51	[23]

To study the transition mechanism in solar cells, excitation density and temperature dependent PL spectroscopy were performed. As shown in Fig. 3(a), PL intensity increases with the excitation laser power. These intensities have been fitted in Fig. 3(b) using the power law:

$$I \propto P^k \quad (2)$$

where P is the excitation power and k is the coefficient. When k $\geqslant$1, the transition recombination is excitonic; When k<1, the transition involves defects recombination.[21] For the CZTS solar cell studied in this work, the fitting in Fig. 3(b) gives a k value of 0.94±0.01, indicating that donor or acceptor defects engage

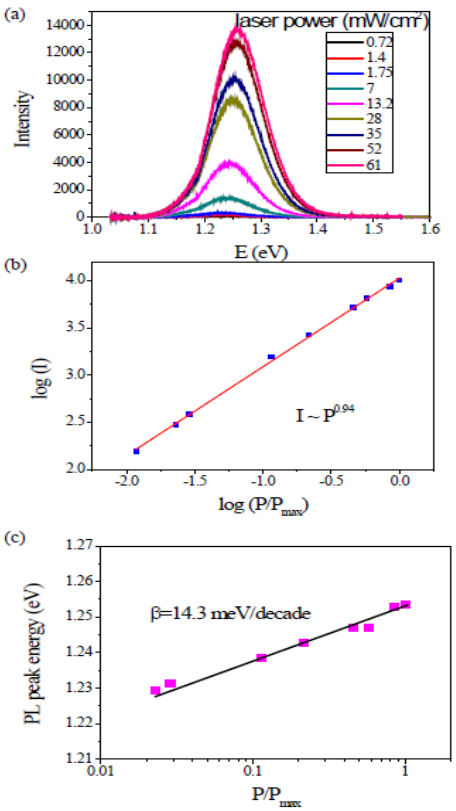

Fig. 3. (a) Power dependent PL spectroscopy of CZTS at 10K. (b) Power law fitting with coefficient of 0.94±0.01. (c) Peak shift as a function of laser power.

in the emission. As shown in Fig. 3(c), a large blue shift of peak energy (~ 25 meV) with slope of 14.3meV/decade is observed when excitation density is increased, which is consistent with previous observations [21,25-28] in solar cell with large potential fluctuations. Actually, the large blue shift with the increasing laser power is one feature of donor-acceptor pair (DAP) transition or band to tail (BT) transition.[21,29] Theoretically, Chen et. al has reported that [Cu_{Zn}^{-}+Zn_{Cu}^{+}] has the lowest formation energy.[30,31]. First-principle calculations[30,31,33] suggest that the activation energies of the acceptor level of Cu_{Zn} and the donor level of Zn_{Cu} are 120 meV and 100 meV, respectively. The observed PL peak shift of 190 meV with respect to its bandgap energy indicates that the observed PL emission can be well attributed to donor-acceptor pairs of Cu_{Zn} and Zn_{Cu}. The large population of charged DAP defects will introduce tail states due to the electrostatic potential fluctuations, of which the fluctuation amplitude is determined by the Coulomb interaction within the medium. CZTS may be expected to have larger fluctuations compared to CIGS considering of the usually observed higher defect density and the smaller relative dielectric constant. Besides the optical behavior, the potential fluctuation or tail states would have strong effect on the carrier transport process in CZTS and CIGS devices. In this work, in addition to the PL technique, we have also used admittance spectra to characterize the effect of potential fluctuation by revealing its trapping process at low temperatures in the absorbers. Both the trapping energy and trap density measured by the admittance measurement will be more directly related to the device performance. The trapping energy will also be very helpful in identifying the possible origin of the defects contributing to the potential fluctuation. From the AS measurement shown in Fig. 4(a) and (b), a trap with activation energy of about 70 meV is observed in the CIGS solar cell. Since the activation energy obtained from the AS measurement is very close to the defect level of V_{Cu} reported by other groups and the acceptor level of V_{Cu} given by the simulation, we therefore attribute the observed luminescence in the CIGS solar cell to the transitions of band to V_{Cu} impurity. The relative small excitation intensity dependence (7 meV/decade) and blue shift of the PL peak energy as the temperature increases also support that the PL emission is band to impurity (BI) transition.[31] The AS measurement of the CZTS sample (Fig. 4(a) and (b)) shows the existence of two kinds of traps with activation energy of 96 meV and 119 meV, respectively. By temperature dependent DLCP measurement, we can readily distinguish that one is an electron trap while another one is a hole trap, which will not be discussed here. These activation energies are very close to the acceptor level of Cu_{Zn} (120 meV) and the donor level of Zn_{Cu} (100 meV) given by the first-principle calculations.[30,31,33] Since the dominant acceptor (Cu_{Zn}) in CZTS has deeper ionization energy than V_{Cu} in CIGS, the ionized acceptor in CZTS will be expected to produce a larger potential fluctuation both in the conduction band and valence band. Furthermore, donors in CIGS did not show pronounced trapping effect which indicated that the electrons in CIGS to be delocalized, while Zn_{Cu} donor in CZTS were found to introduce deep potential traps. From the above observation, we can find that both the ionized donors and ionized deep holes produce potential fluctuations in CZTS, while the potential fluctuation in CIGS are coming from the ionized shallow acceptors only. We have sketched the potential fluctuations in CZTS and CIGS as shown in Fig 4(c) from which one can easily understand that the potential fluctuation will be much pronounced in CZTS by comparing with CIGS. This can partly explain the observed larger V_{oc} deficit in CZTS devices.

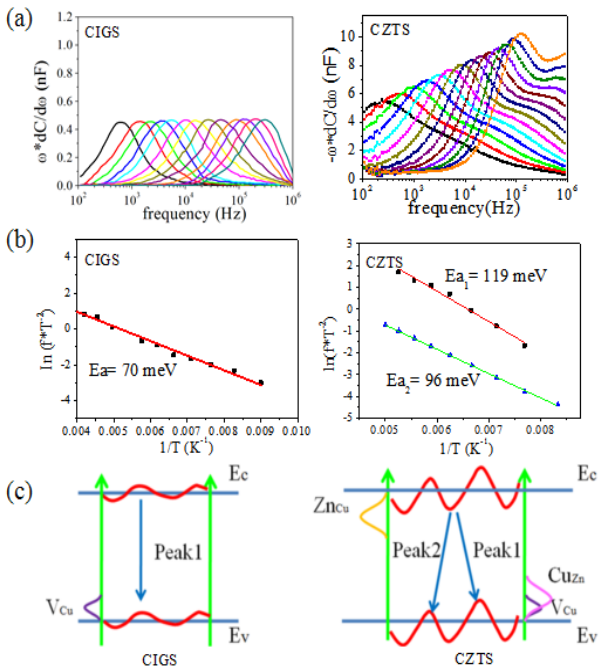

Fig. 4. (a) Admittance spectroscopy of CIGS and CZTS solar cells. (b) Arrhenius plot of the inflection frequencies determined from the derivative of the admittance spectra of CIGS and CZTS solar cells. (c) A schematic diagram of the potential fluctuations and luminescence transitions in CIGS and CZTS.

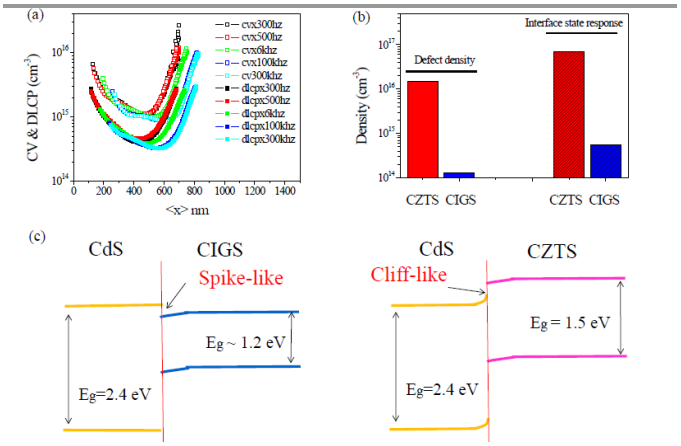

Fig. 5. (a) DLCP of CIGS solar cell (measured at 170K) (DLCP of CZTS solar cell not shown here, refer to Ref [27]) . (b) Defect and interface density of CZTS and CIGS. (c) Schema of the band alignment of CdS/CZTS and CdS/CIGS.

Table 3. Summary of results derived from DLCP measurements of CZTS and CIGS.

Sample	N_t (cm^{-3})	Ni (cm^{-3})	N_f (cm^{-3})
CZTS	1.0×10^{16}	4.0×10^{16}	1.0×10^{16}
CIGS	1.3×10^{14}	5.6×10^{14}	3.2×10^{14}

(N_t: bulk defect density, Ni: interface defect density, N_f: free carrier density)

To further compare the bulk defect density and interface defect density in CTZS and CIGS solar cells, CV and DLCP measurements were used.[15] Since DLCP is insensitive to the response from the interface or near-interface states, we can extract the contribution of the interface states by subtracting the DLCP defect density from the CV defect density. In addition, since the defects cannot respond effectively to the excitation signals at high frequencies, the detected DLCP signal hence provides us the information of free carrier concentration. The measured CV and DLCP of CIGS device at different frequencies are shown in Fig. 5(a). By analyzing the CV and DLCP results, we presented both the bulk trap density and interface defect density in CZTS and CIGS for comparison. Detailed defect density and free carrier density are listed in Table 3. For CZTS, same to previous publication[32], both the bulk defect density and interface defect density are two orders higher than those in the CIGS solar cell. The higher bulk defect density of Cu_{Zn} and Zn_{Cu} with deeper defect level in the CZTS sample will cause larger potential fluctuations, which is also consistent with the PL measurement result. From Table 3, we can find that the interface states density in CZTS is also much higher. There are two possible reasons which can explain the higher interface defect density as observed in the CZTS cell. Firstly, the large lattice misfit between CZTS and CdS (about 7%) may result in interface dislocation/defects and cause minority carrier recombination at the CdS/CZTS interface.[34-35] Secondly, when "cliff-like" band alignment occurs at the CdS/CZTS interface as shown in Fig. 5(c), it is equivalent to an interface band gap reduction which will enhance the recombination, especially for the recombination between electrons in the conduction band of the buffer and holes in the valence band. Due to the high recombination at the CZTS/CdS interface, the V_{oc} of the device will significantly decrease.[34,36] However, we have to say that the formation of "cliff-like" or "spike-like" heterojunction between CdS and CZTS is still an open question.[31,35,37,38]

Based on the above findings, we may conclude that the large V_{oc} deficit which limits the efficiency of the CZTS solar cells is related to both the larger potential fluctuations and higher density interface defects by comparing with CIGS. The potential fluctuation in CZTS is caused by both donors of Zn_{Cu} and acceptors of Cu_{Zn} which have deeper ionization level and much higher population than those of the dominant defect V_{Cu} in CIGS. To make CZTS devcie be with efficiency comparable to CIGS, one has to pay more attention on the defects in the absorber. In addition to optimize the growth parameters to reduce the defect density, it will be with great help to reduce the potential fluctuation if the deep acceptor Cu_{Zn} can be partly replaced by shallow acceptor V_{Cu}. Since the electrons in CZTS also experiences strong localization due to the potential fluctuation introduced by the donors, a design of graded conduction band similar to CIGS will benefit the transport of electrons and thus increase the device efficiency. Band engineering using spatial variation of Se/(S+Se) or Sn/(Ge+Sn) in $Cu_2ZnSn(S,Se)_4$ or $Cu_2Zn(Sn,Ge)Se_4$ will take the advantage of Ga/(Ga+In) grading in CIGS to facilitate the efficient collection of photo-generated electrons.

4. Conclusions

In this work, PL spectroscopy, DLCP, and AS measurement were used to characterize the factors limiting the performance of the CZTS solar cell by comparing with CIGS. Our results suggest that deep defect energy of acceptor Cu_{Zn} and donor Zn_{Cu}, and resulting large potential fluctuation of the band structure, together with high density of interface defects cause the limitation of the efficiency of CZTS solar cell. The potential fluctuation in CIGS comes mainly from the dominant shallow acceptor V_{Cu}. Optimizing the growth parameters to suppress the deep Cu_{Zn} defect and to increase the advantageous V_{Cu} will possibly reduce the resulting potential fluctuation. To overcome the potential fluctuation induced trapping effect for electrons by the Zn_{Cu} donors, we suggest that a graded conduction band similar to CIGS will be a good solution to eliminate electron localization.

Acknowledgements

This work is supported by 973 project of China under 2012CB933700, NSF of China under 61274093 and 51302304, 51302303. We will also thank ITC funding of Shen Zhen under projects KQC201109050091A and JCYJ20120617151835515.

Notes and references

1. Y. B. K. Kumar, G. S. Babu, P. U. Bhaskar and V. S. Raja, *Solar Energy Materials and Solar Cells*, 2009, **93**, 1230-1237.
2. D. B. Mitzi, O. Gunawan, T. K. Todorov, K. Wang and S. Guha, *Solar Energy Materials and Solar Cells*, 2011, **95**, 1421-1436.
3. N. Yu, R. Z. Zhong, W. J. Zhong, X. L. Chen, J. Luo, X. D. Gu, X. H. Hu, L. S. Zhang, J. Q. Hu and Z. G. Chen, *RSC Adv.*, 2014, **4**, 36046–36052.
4. K. Ito and T. Nakazawa, *Japanese Journal of Applied Physics*, 1988, **27**, 2094-2097.
5. K. Jimbo, R. Kimura, T. Kamimura, S. Yamada, W.S. Maw, H. Araki, K. Oishi and H. Katagiri, *Thin Solid Films*, 2007, **515**, 5997-5999.
6. H. Katagiri, K. Jimbo, S. Yamada, T. Kamimura, W.S. Maw, T. Fukano, T. Ito and T. Motohiro, *Appl. Phys. Express*, 2008, **1**, 41201-1-2.
7. A. Ennaoui, M. Lux-Steiner, A. Weber, D. Abou-Ras, I. Kötschau, H.-W. Schock, R. Schurr, A. Hölzing, S. Jost, R. Hock, T. Voß, J. Schulze and A. Kirbs, *Thin Solid Films*, 2009, **517**, 2511-2514.

8. J. Madarász, P. Bombicz, M. Okuya and S. Kaneko, *Solid State Ionics*, 2001, **141–142**, 439–446.
9. T. Todorov, O. Gunawan, S.J. Chey, T.G. Monsabert, A. Prabhakar and D.B. Mitzi, *Thin Solid Films*, 2011, **519**, 7378-7381.
10. W. Wang, M. T. Winkler, O. Guanwa, T. Gokmen, T. K. Godorov, Y. Zhu and D. B. Mizi, *Adv. Energy Mater.*, 2014, **4**, 1301465.
11. T. Kato, H. Hiroi, N. Sakai, S. Muraoka, H. Sugimoto, 27th European Photovoltaic Solar Energy Conference, 2012, DOI: 10.4229/27thEUPVSEC2012-3CO.4.2.
12. ZSW press release, Stuttgart, September 22, 2014.
13. T. Gokmen, O. Gunawan, T. K. Todorov and D. B. Mitzi, *Appl. Phys. Lett.*, 2013, 103, 103506-1-5.
14. K. Tanaka, T. Shinji, H. Uchiki, *Solar Energy Materials and Solar Cells*, 2014, **126**, 143-148.
15. E. O. Kane, *Phys. Rev*., 1963, **131**, 79-88.
16. S. Siebentritta, N. Papathanasioua, and M.Ch. Lux-Steine, *Physica B*, 2006, **376-377**, 831-833.
17. J. H. Werner, J. Mattheis, U. Rau, *Thin Solid Films*, 2005, **480–481**, 399– 409.
18. T. Gershon, B. Shin, T. Gokmen, S. Lu, N. Bojarczuk, and S. Guha, *Appl. Phys. Lett.*, 2013, 103, 193903-1-3.
19. J. T. Heath , J. D. Cohen and W. N. Shafarman, J. Appl. Phys., 2004 95 , 1000-1010 .
20. J. Mattheis, U. Rau, and J. H. Werner, *J. Appl. Phys.* 2007, 101, 113519.
21. D. P. Halliday, R. Claridge, M. C. J. Goodman, B. G. Mendis, K. Durose and J. D. Major, *J. Appl. Phys.*, 2013, **113**, 223503-1-10.
22. J. Krustok, J. Raudoja, M. Yakushev, R.D. Pilkington and H. Collan , *Phys. Status Solidi*, 1999, **173**, 483-490.
23. J. Krustok, H. Collan, M. Yakushev and K. Hjelt, *Physica Scripta*, 1999, **79**, 179-182.
24. I. Dirnstorfer, Mt. Wagner, D.M. Hofmann, M.D. Lampert, F. Karg and B.K. Meyer, *phys. stat. sol.*, 1998, **168**, 163-175.
25. M. Grossberg, J. Krustok, A. Jagomägi, M. Leon, E. Arushanov, A. Nateprov and I. Bodnar, *Thin Solid Films*, 2007, **515**, 6204–6207.
26. J.P. Leitão, N.M. Santos, P.A. Fernandes, P.M.P. Salomé, A.F. da Cunha, J.C. González, G.M. Ribeiro, F.M. Matinaga, *Phys. Rev. B*, 2011, **84**, 024120-1-8.
27. K. Tanaka, Y. Miyamoto, H. Uchiki, K. Nakazawa, H. Araki, *phys. stat. sol.*, 2006, **203**, 2891– 2896.
28. L. Van Puyvelde, J. Lauwaert, P.F. Smet, S. Khelifi, T. Ericson, J.J. Scragg, D. Poelman, R. Van Deun, C. Platzer-Björkman and H. Vrielinck, *Thin Solid Films*, 2014, doi:10.1016/j.tsf.2014.10.079.
29. M. Grossberg, P. Salu, J. Raudoja and J. Krustok, 2013, **3**, 030599-1-6.
30. S. Y. Chen , A. Walsh , X. G. Gong and S. H. Wei, *Adv. Mater.* 2013, **25**, 1522–1539.
31. S. Y. Chen, J. H. Yang, X. G. Gong, A. Walsh and S. H. Wei, *PHYSICAL REVIEW B*, 2010, **81**, 245204-1-10.
32. G. M. Cheng, Y. Feng, Z. H. Li, L. Yin, X. D. Xiao, C. L. Yang. Defect study of CZTS solar cells by admittance spectroscopy, submitted.
33. A. Walsh, S. Y. Chen , S. H. Wei and X. G. Gong, *Adv. Energy Mater.* , 2012, **2**, 400–409.
34. W. Li, J. Chen, C. Yan and X. J. Hao, *Journal of Alloys and Compounds*, 2015, 632, 178-184.
35. A. Nagoya, R. Asahi, G. Kresse, *J. Phys.: Condens. Matter*, 2011, 23 404203.
36. T. Minemoto, T. Matsui, H. Takakura, Y. Hamakawa, T. Negami, Y. Hashimoto, T. Uenoyama T and M. Kitagawa, *Solar Energy Materials an Solar Cells*, 2001, 67, 83-88.
37. M. Bar, B. A. Schubert, B. Marsen, R. G. Wilks, S. Pookpanratana, M. Blum, S. Krause, T. Unold, W, Yang, L. Weinhardt, C. Heske, and H. W. Schock, *Appl. Phys. Lett.*, 2011, 99, 222105-1-3.
38. R. Haight, A. Barkhouse, O. Gunawan, B. Shin, M. Copel, M. Hopstaken and D. B. Mitzi, *Appl. Phys. Lett.*, 2011, 98, 253502.

Table of contents entry

Limitation factors for the performance of kesterite Cu2ZnSnS4 thin film solar cells studied by defects characterization

Ling Yin,[ab] Guanming Cheng,[b] Ye Feng,[b] Zhaohui Li,[b] Chunlei Yang,*[b] Xudong Xiao*[ab]

[a] *Department of Physics, The Chinese University of Hong Kong, Shatin, Hong Kong, China*

[b] *Center for Photovoltaics Solar Energy, Shenzhen Institutes of Advanced Technology, Chinese Academy of Sciences, Shenzhen, 518055, China*

Table of contents entry

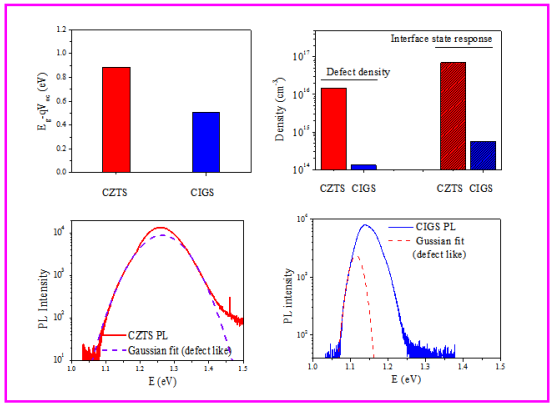

PL, AS and DLCP have been performed to study the limitation factors for the performance of CZTS solar cells.